Nonlinearities in patterns of long term ocean warming

Maria Rugenstein,[1] Jan Sedláček,[1] Reto Knutti,[1]

Corresponding author: M. Rugenstein, Institute for Atmospheric and Climate Science, ETH Zürich, Universitätstrasse 16, 8092 Zürich, Switzerland. (maria.rugenstein@env.ethz.ch)

[1]Institute for Atmospheric and Climate Science, ETH Zürich, Universitätstrasse 16, 8092 Zürich, Switzerland

Key Points.

- Response time scales and regions of ocean heat uptake depend non-linearly on the forcing level.
- Global thermal expansion does not scale linearly with the surface temperature anomaly.
- Reasons are forcing dependent circulation responses and the non-linear equation of state.

The ocean dominates the planetary heat budget and takes thousands of years to equilibrate to perturbed surface conditions, yet those long time scales are poorly understood. Here we analyze the ocean response over a range of forcing levels and time scales in a climate model of intermediate complexity and in the CMIP5 model suite. We show that on century to millennia time scales the response time scales, regions of anomalous ocean heat storage, and global thermal expansion depend non-linearly on the forcing level and surface warming. As a consequence, it is problematic to deduce long term from short term heat uptake or scale the

heat uptake patterns between scenarios. These results also question simple methods to estimate long term sea level rise from surface temperatures, and the use of deep sea proxies to represent surface temperature changes in past climate.

1. Centennial scale ocean heat uptake in CMIP5 models

Thermal expansion of ocean waters due to heat uptake from the atmosphere is a large contributor to recent and near future sea level rise [*Church et al.*, 2011, 2013; *Levermann et al.*, 2013]. General circulation models (GCM) differ in the amplitude of simulated thermal expansion due to different base states, the total amount and vertical extent of the heat uptake, heat redistribution, and differences in the representation of vertical heat transport processes, advection, isopycnal and diapycnal mixing [*Gregory*, 2000; *Kuhlbrodt and Gregory*, 2012; *Hallberg et al.*, 2012; *Church et al.*, 2013; *Exarchou et al.*, 2014; *Melet and Meyssignac*, 2015; *Liang et al.*, 2015]. Fig. 1a-c shows zonal averaged ocean temperature anomaly patterns at the end of the century for three different scenarios simulated by the Coupled Model Intercomparison Project Phase 5 (CMIP5) models. 95-97% of the ocean heat uptake is confined to the upper kilometer, although locally, deep ocean heat uptake can contribute a large fraction of the total amplitude already decades after the perturbation [*Kuhlbrodt and Gregory*, 2012; *Marshall et al.*, 2014]. The standard deviation between the models increases with the forcing level and in Southern and Northern hemispheric high latitudes, but is generally smaller in magnitude than the mean signal shown in Fig. 1, see also Supplemental Information (SI) Fig. 1-3 [*Yin*, 2012; *Sallée et al.*, 2013; *Heuzé et al.*, 2015]. Fig. 1d-e demonstrate that locally, pattern scaling between the different scenarios is not possible with high accuracy [*Bilbao et al.*, 2015]. If the ocean warming pattern would respond linearly to the surface forcing the differences between the scaled scenarios in the upper row should be zero. However, the lower forced scenario takes up relatively more heat into the Southern Ocean and to low latitude intermediate depth

of around 500 – 2000m (panel d) than the intermediate and higher forced scenarios (panel f). In the surface ocean higher forcing lead to relatively more heat uptake (see also SI Fig. 1 for a zoom into the upper ocean).

The near future sea level rise has been studied extensively, but is also known to be a poor indicator of centennial, millennial, or equilibrated conditions [e.g., *Stouffer and Manabe*, 2003; *Li et al.*, 2013], but only very few GCMs have been run over millennia due to computational cost. Here we explore the centennial to millennia patterns of ocean warming and their dependence on time and on forcing levels. We show that long term thermal expansion is not proportional to surface warming, and that deduction of one time frame or forcing scenario to another is limited, not only for the transient response as shown for the CMIP5 models, but also for equilibrated conditions.

2. Model and Simulations

To explore the limits of scaling over a wide range of forcing levels and timescales up to equilibrium, we use the intermediate complexity model (EMIC) ECBILT-CLIO, which consists out of an ocean, sea ice, and atmospheric component. The ocean general circulation model has a free surface, 20 unevenly spaced layers, a 3°x3° horizontal resolution, and a thermodynamic-dynamic sea ice model [*Goosse and Fichefet*, 1999, and more details on the model formulation in the SI]. The atmospheric model solves the quasi-geostrophic equations on a spectral grid with three vertical levels and a horizontal resolution of 5.6°x5.6°, parameterizations of diabatic heating and surface heat fluxes, and prescribed seasonal varying cloud cover [*Opsteegh et al.*, 2011]. This results in a low Equilibrium Climate Sensitivity (ECS) of 1.7 K [see also *Friedrich et al.*, 2010; *Levermann et al.*, 2013;

Eby et al., 2013; *Church et al.*, 2013, and references therein]. Given the limitations of the model, we emphasize that we aim at insight and not prediction. We will interpret the scenarios relative to each other, rather than their absolute values compared to other models with the same forcing. The advantage of the model is that large ensembles of hundreds of members, and simulations of 10,000 years are possible, a range unfeasible with a full general circulation model.

We conduct a range of step forcing experiments, each consisting – roughly according to the ratio of anomaly signal to internal variability noise – of several initial condition ensemble members: 1.07 times preindustrial CO_2 concentrations of 280ppm (90 members), 1.4xCO_2 (90 members), 2xCO_2 (50 members), 4xCO_2 (20 members), 8xCO_2 (20 members), and 16xCO_2 (10 members), each 1000 years long. The forcing levels are chosen to simulate roughly no change in circulation for the very low forced cases to an initially strongly stratified response and large heat uptake for the high forced cases. One member of each forcing level is further integrated to 10,000 years. We show anomalies of these simulations with 1000 or 10,000 year long control simulations (no CO_2 change, 94 initial condition ensemble members), i.e. each ensemble member's anomaly is determined with a slightly different control simulation. The temperature of the control simulations shows no drift, but the salinity shows both a small linear control run drift (globally $0.05\,\mathrm{kg\,m^{-3}}$ per 10,000 yrs) and a smaller forcing level dependent drift, due to the handling of the sea ice. Both drifts are accounted for by scaling the salinity pattern at each time step, location, and forcing level with the drift, so that the global mean salinity is constant at all times, but allowed to change its spatial pattern.

3. Equilibration of ocean heat uptake and circulation changes

Fig. 2 a-d shows – analogous to Fig. 1 – the equilibrium zonally averaged ocean temperature anomalies normalized with the equilibrium global ocean temperature for four representative scenarios in color, and the unscaled changes in salinity in grey contours. The temperature anomaly is not distributed homogeneously even though the global ocean temperature is in equilibrium with the surface. This agrees with models showing gradients of several degrees (*Gillett et al.* [2011] and *Knutti* [2002]), but disagrees with the rather homogeneous warming patterns of *Stouffer and Manabe* [2003] and *Li et al.* [2013], in which the vertical gradient of temperature is less than 1.5 K. Contrary to the transient pattern analyses of *Kuhlbrodt and Gregory* [2012] and *Melet and Meyssignac* [2015], the equilibrated simulations do not scale with their global temperature especially in the Southern Ocean, which is widely recognized to be important in shaping the transient and equilibrium global heat uptake [e.g., *Schneider and Thompson*, 1981; *Manabe and Stouffer*, 1994; *Bi et al.*, 2001; *Bryan et al.*, 2006]. The Northern Hemisphere high latitudes become relatively more important in lower forced scenarios, as suggested also in Fig. 1 d-f. Salinity and temperature anomalies roughly follow the same pattern, but impact the density in opposite ways through the equation of state. In regions with increased warming, the salinity anomaly is positive, thus compensating the change in density due to the increased heat content [*Lowe and Gregory*, 2006]. This explains why the maximum warming can be sustained in the tropical subsurface ocean without destabilizing the water column [*Yin et al.*, 2011]. Panels e-h show the time evolution of global ocean warming with depth. While the higher forced scenarios take longer to equilibrate they are more efficient

in transporting the anomaly into the deep ocean. However, taking the average subsurface maximum versus deep ocean temperature as an indicator of homogeneity, we find that the vertical gradient does not evolve linearly with the forcing level: The subsurface maximum warming is a factor of 3.3, 5, 7, 4.3, 1.9, and 1.2 greater than the deep ocean warming for the scenarios of 1.07, 1.4, 2, 4, 8, 16xCO_2. On century time scales, for very low forced scenarios even negative deep ocean temperature trends are possible (panel e blue lines). This is consistent with slightly decreasing trends in recent decadal observations [*Wunsch and Heimback*, 2014; *Llovel et al.*, 2014; *Liang et al.*, 2015]. Locally, slightly negative and positive trends can occur after the upper 2000m are fully equilibrated.

Fig. 3 further explains the time evolution of the different forcing scenarios. All panels share the same color coding (ranging from 1.07 in yellow to 16xCO_2 in blue) and logarithmic time axis. The global average surface air temperature anomaly (panel a) scales only roughly with the forcing level (i.e., the equilibrium climate sensitivity for higher forcings is less than expected from linearly scaling up lower forcing levels). Panel b shows the global average ocean temperature anomaly with the global value as solid and the upper most kilometer evolution as dashed lines. In some scenarios, the deep ocean reaches its equilibrium value at almost the same time scale as the upper ocean (4xCO_2), while for other scenarios it takes several thousand years longer (8xCO_2), dependent on stratification, overturning, and mixing response. Panel c depicts the sea level rise due to ocean thermal expansion and salinity changes, calculated from the global detrended in-situ density anomaly, volume, control run reference density and surface area. The gray dashed lines show the sea level rise due to thermal expansion only, assuming a constant salinity

pattern. While locally the salinity changes are important to set the dynamics and sea level change, globally they are negligible. In equilibrium, the deep ocean (below 1km) accounts for 64, 55, 60, 67, and 72 % of the total thermal expansion for the 1.07, 1.4, 2, 4, and 16xCO_2 forcing, respectively. This compares well with the 60% contribution of the deep (below 1.5km) ocean of the general circulation model of *Li et al.* [2013].

The patterns of ocean heat uptake and redistribution, as well as changes in the patterns of salinity depend on circulation changes, thus on surface temperature anomaly and the forcing level. The Atlantic Meridional Overturning Circulation (AMOC, panel d), here defined as the maximum in the stream function at 30° N, initially declines, as expected, more with a higher forcing level [*Manabe and Stouffer*, 1994; *Gregory et al.*, 2005; *Zhu et al.*, 2014]. However, both the recovery level and recovery rate vary with the forcing level and some scenarios recover to a greater degree than others. While almost all GCMs and EMICs show a reduction of the AMOC with increased radiative forcing, the time and strength of the recovery differs strongly between them [*Stouffer and Manabe*, 2003; *Li et al.*, 2013; *Zickfeld et al.*, 2013]. The recovery or increased instability can be caused by a surface salt-advection feedback [*Latif et al.*, 2000; *Bryan et al.*, 2013] or increased bottom water temperatures due to slower Antarctic Bottom Water Formation (AABWF) [*Manabe and Stouffer*, 1994; *Stouffer and Manabe*, 2003]. Since the stronger the AMOC declines, the more heat can be taken up by the deep North Atlantic [*Rugenstein et al.*, 2013], the very strong reduction and slow recovery in the higher forced cases likely causes the more vertically homogeneous equilibrium temperature anomaly (Fig. 2).

Finally, panel e and f show the time evolution the AABWF strength – defined as maximum overturning at 70° S – and the sea ice volume – depicted as fraction of the control run value. The AABWF reduces in all cases, but does not scale linearly with the radiative forcing. The time of minimum AABWF, the recovery or overshooting amplitude, and rate of recovery vary several thousand years between the different forcing cases. The reason for the recovery is not well understood and attributable to either the long-term warming or the salinization of the deep ocean, destabilizing the water column from below [*Manabe and Stouffer*, 1994; *Bi et al.*, 2001], or strong enough convective events triggered by changed seasonality [*Yamamoto et al.*, 2015]. The higher forced levels, which show relatively more deep ocean warming (Fig. 2), indeed recover and overshoot. The Southern Ocean sea ice reduces in all cases roughly proportional to the forcing level until year 20, before the rate of change as well as the equilibrium level becomes forcing level dependent.

4. Thermal expansion

We now explore the consequences of the in-homogeneous and forcing dependent warming pattern on the sea level rise due to thermal expansion. Previous studies used the equilibrium surface temperature anomaly as dependent variable and found an approximately linear relation to the thermal expansion [*Knutti and Stocker*, 2000; *Meehl et al.*, 2007; *Levermann et al.*, 2013], but the evidence for this is mostly based on intermediate complexity, 2.5D, or single basin models. However, there is no physical reason why this should be the case, and *Pardaens et al.* [2011] and *Körper et al.* [2013] find indeed, but do not explain, non-linearities for transient states at the end of the century for several GCMs. We discuss three mechanisms which impact the relationship between the thermal

expansion and surface temperature anomaly (Fig. 4). (1) The non-linearity of the equation of state: The expansion coefficient of sea water increases with warmer temperature and lower pressure [e.g., *Palter et al.*, 2014]. (2) The transient effects of taking up more heat with time but moving a larger fraction of heat into the deep ocean, where thermal expansion is less. (3) The forcing level and circulation dependent heat uptake as discussed in Fig. 2 and 3. *Knutti and Stocker* [2000] pointed out that thermal expansion is 0.5 m higher with a shutdown AMOC compared to a state of the same forcing and recovered AMOC or North Pacific overturning. We reproduce this result in ECBILT-CLIO through a fresh water perturbation in the North Atlantic and the sea level rise due to the AMOC collapse – without any radiative forcing – is 0.3 m.

To fill up gaps between simulations shown above and to explore higher warming levels, we show 18 additional simulations (depicted by dots in Fig. 4). The lowest forcing is 1.15xCO_2 (dots farthest left), increasing in steps of $2^{0.2}$ up to $2^{4.4} = 21$xCO_2 (dots on the far right). The surface temperature sensitivity even becomes lower at high CO_2 values, so 21xCO_2 should not be interpreted at face value. The time dimension is depicted in colors, showing five decadal to millennia time slices. Fig. 4a and b show that the total ocean heat uptake (which dominates the Top of the Atmosphere (TOA) radiative imbalance), is linearly related to the surface air temperature anomaly at all times, but does not translate into a linear relationship between the ocean and surface air temperature anomalies on centennial to millennial time scales. For one unit of surface warming the ocean warms more through time (equilibration, curves moving up) and higher forcing levels (circulation changes, curves bend up, see also Fig. 2 and 3). Fig. 4c brings the

equation of state into play: The sea level rise due to thermal expansion is linearly related to the ocean temperature anomaly on decadal time scales (dark red line). If the equation of state were linear and the circulation was constant, the equilibrium values would lie on the black line, far away from the equilibrated model output (green line). To assess how much of this non-linearity is due to the equation of state, we use the 3D warming and salinity pattern after 50 years and linearly scale it up, mimicking 5K more warming under the assumption of no circulation change. We then calculate the thermal expansion with the non-linear equation of state (*McDougall et al.* [2003], rho_mwif function, see also SI, gray dashed line). The green line is close to that estimate, i.e., the greatest part of the non-linearity of the equilibrated situation is due to the fact that the equation of state is non-linear. The remaining discrepancy between the gray and green line is due to the effect that for longer time scales and higher forcing levels more heat is transported from the surface layers to the deep ocean. Fig. 4d brings all effects together, showing that thermal expansion from centennial time scales onwards – increasingly with higher forcing levels – is non-linearly related to the surface temperature anomaly. The dashed gray lines show again two artificially constructed cases to assess the impact of the non-linear equation of state without circulation changes (explained in the SI). In summary, thermal expansion is approximately proportional to the atmospheric warming on timescales of a century and for small forcings, but on long timescales or for stronger forcings the linearity assumption is no longer valid. The reasons are that the globally integrated heat uptake itself is not proportional to surface warming and that the distribution of warming changes

with changes in circulation and mixing, which in combination with the nonlinearity of the equation of states affects thermal expansion.

5. Implications for paleo and modern studies

A common assumption in paleo oceanography is that the temperature (anomaly) of the intermediate or deep ocean – indicated by e.g. benthic foraminifera – represents a time averaged (sea) surface temperature (SST) record of the regions where deep waters formed [e.g., *Savin*, 1977; *Huber*, 1998; *Zachos et al.*, 2001; *Voigt et al.*, 2004; *Cramer et al.*, 2009; *Friedrich et al.*, 2012] or the SST anomalies represent deep ocean temperature anomalies [*Jaccard et al.*, 2014]. Modeling studies found the deep water temperature anomaly was the same as the southern high latitude SST anomaly [*Manabe and Bryan*, 1985] or that it resembles the SST anomaly of low latitude [*Stouffer and Manabe*, 2003]. We find that the anomalous heat uptake by the intermediate and deep ocean does not correspond to the atmospheric temperature increase at low or high latitudes. This implies that, without knowledge of forcing and circulation history, the interpretation of ocean temperature proxies beyond their region may be more problematic than currently appreciated. Another long term implication of our finding concerns climate sensitivity. Fig. 3a indicates that the effective climate sensitivity in the model increases with increased temperatures for all simulations (see more elaborate argument in *Knutti and Rugenstein* [2015]). This implies that potentially, ocean circulation can have a large effect on the TOA radiative imbalance even in the absence of a cloud feedback. A more general consequence concerns the marine carbon-climate feedback and regions of melting sea ice, which both are likely influenced by the places of anomalous heat storage and thus, dependent on the forcing

history [*Randerson et al.*, 2015]. Finally and also on shorter timescales, pattern scaling between scenarios might break down already at the end of this century, or more likely in future centuries. We therefore cannot infer future or past equilibria from transient behavior or past transient behavior from equilibria. A detailed knowledge of the dependence of circulation responses to different forcing levels and scenarios is key to understand and compare not only transient, but also equilibrium warming patterns.

In summary, although for sub-centennial time scales and low forcing levels the linear relationship between thermal expansion and surface temperature anomaly seems to hold, our analysis suggests that we do not properly understand the centennial to millennia ocean warming patterns, mainly due to a limited understanding of circulation and mixing changes. Complex enough models – simulating long enough time scales and different ranges of scenarios (as e.g., in *Krasting et al.* [2016])– are necessary to explore these effects.

Acknowledgments. We thank Thomas Frölicher, Axel Timmermann, Summer Praetorius, and two anonymous reviewers for comments and discussions. We acknowledge the World Climate Research Programme's Working Group on Coupled Modelling, which is responsible for CMIP, and we thank the climate modeling groups (listed in Fig.S3 of the SI) for producing and making available their model output. For CMIP the U.S. Department of Energy's Program for Climate Model Diagnosis and Intercomparison provides coordinating support and led development of software infrastructure in partnership with the Global Organization for Earth System Science Portals. Data from the EMIC used

here are available upon requested from the authors. ECBILT–CLIO is free to download from KNMI at http://www.sciamachy-validation.org/research/CKO/ecbilt.html.

References

Bi, D., W. F. Budd, A. C. Hirst, and X. Wu (2001), Collapse and reorganisation of the Southern Ocean overturning under global warming in a coupled model, *Geophysical Research Letters*, *28*(20), 3927–3930, doi:10.1029/2001GL013705.

Bilbao, R. A., J. M. Gregory, and N. Bouttes (2015), Analysis of the regional pattern of sea level change due to ocean dynamics and density change for 1993–2099 in observations and CMIP5 AOGCMs, *Climate Dynamics*, *45*(9-10), 2647–2666, doi:10.1007/s00382-015-2499-z.

Bryan, F., N. Nakashiki, Y. Yoshida, and K. Maruyama (2013), Response of the Meridional Overturning Circulation During Differing Pathways Toward Greenhouse Gas Stabilization, in *Ocean Circulation: Mechanisms and Impacts—Past and Future Changes of Meridional Overturning*, edited by A. Schmittner, J. C. H. Chiang, and S. R. Hemming, pp. 351–363, American Geophysical Union, doi:10.1029/173GM22.

Bryan, F. O., G. Danabasoglu, N. Nakashiki, Y. Yoshida, D.-H. Kim, J. Tsutsui, and S. C. Doney (2006), Response of the North Atlantic Thermohaline Circulation and Ventilation to Increasing Carbon Dioxide in CCSM3, *Journal of Climate*, *19*(11), 2382–2397, doi:10.1175/JCLI3757.1.

Church, J. A., N. J. White, L. F. Konikow, C. M. Domingues, J. G. Cogley, E. Rignot, J. M. Gregory, M. R. van den Broeke, A. J. Monaghan, and I. Velicogna (2011), Revisiting the Earth's sea-level and energy budgets from 1961 to 2008, *Geophysical Research*

Letters, *38*(18), doi:10.1029/2011GL048794.

Church, J. A., P. U. Clark, A. Cazenave, J. M. Gregory, S. Jevrejava, A. Levermann, M. Merrifield, G. Milne, R. Nerem, P. Nunn, A. J. Payne, W. T. Pfeffer, D. Stammer, and A. Unnikrishnan (2013), Sea Level Change, in *Climate Change 2013: The Physical Science Basis. Contribution of Working Group I to the Fifth Assessment Report of the Intergovernmental Panel on Climate Change*, edited by T. Stocker, D. Qin, G.-K. Plattner, M. Tignor, S. K. Allen, J. Boschung, A. Nauels, Y. Xia, V. Bex, and P. Midgley, Cambridge University Press.

Collins, M., R. Knutti, J. M. Arblaster, J.-L. Dufresne, T. Fichefet, P. Friedlingstein, X. Gao, T. Gutowski, G. Johns, G. Krinner, M. Shongwe, C. Tebaldi, A. Weaver, and M. F. Wehner (2013), Long-term Climate Change: Projections, Commitments and Irreversibility, in *Climate Change 2013: The Physical Science Basis. Contribution of Working Group I to the Fifth Assessment Report of the Intergovernmental Panel on Climate Change*, edited by T. Stocker, D. Qin, G.-K. Plattner, M. Tignor, S. K. Allen, J. Boschung, A. Nauels, Y. Xia, V. Bex, and P. Midgley, Cambridge University Press.

Cramer, B. S., J. R. Toggweiler, J. D. Wright, M. E. Katz, and K. G. Miller (2009), Ocean overturning since the Late Cretaceous: Inferences from a new benthic foraminiferal isotope compilation, *Paleoceanography*, *24*(4), doi:10.1029/2008PA001683.

Eby, M., A. J. Weaver, K. Alexander, K. Zickfeld, A. Abe-Ouchi, A. A. Cimatoribus, E. Crespin, S. S. Drijfhout, N. R. Edwards, A. V. Eliseev, G. Feulner, T. Fichefet, C. E. Forest, H. Goosse, P. B. Holden, F. Joos, M. Kawamiya, D. Kicklighter, H. Kienert, K. Matsumoto, I. I. Mokhov, E. Monier, S. M. Olsen, J. O. P. Pedersen, M. Perrette,

G. Philippon-Berthier, A. Ridgwell, A. Schlosser, T. Schneider von Deimling, G. Shaffer, R. S. Smith, R. Spahni, A. P. Sokolov, M. Steinacher, K. Tachiiri, K. Tokos, M. Yoshimori, N. Zeng, and F. Zhao (2013), Historical and idealized climate model experiments: an intercomparison of earth system models of intermediate complexity, *Climate of the Past*, *9*(3), 1111–1140, doi:10.5194/cp-9-1111-2013.

Exarchou, E., T. Kuhlbrodt, J. M. Gregory, and R. S. Smith (2014), Ocean heat uptake processes: A model intercomparison, *Journal of Climate*, *28*(2), 887–908, doi:10.1175/JCLI-D-14-00235.1.

Friedrich, O., R. D. Norris, and J. Erbacher (2012), Evolution of middle to Late Cretaceous oceans-A 55 m.y. record of Earth's temperature and carbon cycle, *Geology*, *40*(2), 107–110, doi:10.1130/g32701.1.

Friedrich, T., A. Timmermann, L. Menviel, O. Elison Timm, A. Mouchet, and D. M. Roche (2010), The mechanism behind internally generated centennial-to-millennial scale climate variability in an earth system model of intermediate complexity, *Geoscientific Model Development*, *3*(2), 377–389, doi:10.5194/gmd-3-377-2010.

Gillett, N. P., V. K. Arora, K. Zickfeld, S. J. Marshall, and W. J. Merryfield (2011), Ongoing climate change following a complete cessation of carbon dioxide emissions, *Nature Geosci*, *4*(2), 83–87.

Goosse, H., and T. Fichefet (1999), Importance of ice-ocean interactions for the global ocean circulation: A model study, *Journal of Geophysical Research: Oceans*, *104*(C10), 23,337–23,355, doi:10.1029/1999JC900215.

321 Gregory, J. M. (2000), Vertical heat transports in the ocean and their effect on time-
322 dependent climate change, *Climate Dynamics*, *16*, 501–515, 10.1007/s003820000059.

323 Gregory, J. M., K. W. Dixon, R. J. Stouffer, A. J. Weaver, E. D. M. Eby, T. Fichefet,
324 H. Hasumi, A. Hu, J. H. Jungclaus, I. V. Kamenkovich, A. Levermann, M. Montoya,
325 S. Murakami, S. Nawrath, A. Oka, A. P. Sokolov, and R. B. Thorpe (2005), A model
326 intercomparison of changes in the Atlantic thermohaline circulation in response to in-
327 creasing atmospheric CO_2 concentration., *Geophys. Res. Lett.*, *32*(L12703).

328 Hallberg, R., A. Adcroft, J. P. Dunne, J. P. Krasting, and R. J. Stouffer (2012), Sensitivity
329 of twenty-first-century global-mean steric sea level rise to ocean model formulation,
330 *Journal of Climate*, *26*(9), 2947–2956, doi:10.1175/JCLI-D-12-00506.1.

331 Heuzé, C., K. J. Heywood, D. P. Stevens, and J. K. Ridley (2015), Changes in Global
332 Ocean Bottom Properties and Volume Transports in CMIP5 Models under Climate
333 Change Scenarios, *Journal of Climate*, *28*(8), 2917–2944, doi:10.1175/JCLI-D-14-
334 00381.1.

335 Huber, B. T. (1998), Tropical Paradise at the Cretaceous Poles?, *Science*, *282*(5397),
336 2199–2200, doi:10.1126/science.282.5397.2199.

337 Jaccard, S., E. D. Galbraith, T. L. Frölicher, and N. Gruber (2014), Ocean
338 (de)oxygenation across the last deglaciation: Insights for the future., *Oceanography*,
339 *27*(1), 26–35.

340 Knutti, R. (2002), Modelling studies on the probability and predictability of future climate
341 change, Ph.D. thesis, Physics Institute, University of Bern, 138pp.

342 Knutti, R., and M. A. A. Rugenstein (2015), Feedbacks, climate sensitivity and the limits
343 of linear models, *Philosophical Transactions of the Royal Society of London A: Mathe-*
344 *matical, Physical and Engineering Sciences*, *373*(2054), doi:10.1098/rsta.2015.0146.
345 Knutti, R., and T. F. Stocker (2000), Influence of the Thermohaline Circulation on
346 Projected Sea Level Rise, *Journal of Climate*, *13*(12), 1997–2001, doi:10.1175/1520-
347 0442(2000)0131997:IOTTCO2.0.CO;2.
348 Körper, J., I. Höschel, J. Lowe, C. Hewitt, D. Salas y Melia, E. Roeckner, H. Huebener, J.-
349 F. Royer, J.-L. Dufresne, A. Pardaens, M. Giorgetta, M. Sanderson, O. Otterå, J. Tjiputra, and S. Denvil (2013), The effects of aggressive mitigation on steric sea level rise and
351 sea ice changes, *Climate Dynamics*, *40*(3-4), 531–550, doi:10.1007/s00382-012-1612-9.
352 Kuhlbrodt, T., and J. Gregory (2012), Ocean heat uptake and its consequences
353 for the magnitude of sea level rise and climate change, *Geophys. Res. Lett.*, doi:
354 10.1029/2012GL052952.
355 Krasting, J. P., J.P. Dunne, R.J. Stouffer, and R.W. Hallberg (2016), Enhanced Atlantic
356 sea-level rise relative to the Pacific under high carbon emission rates, *Nature Geosci*,
357 doi:10.1038/ngeo2641.
358 Latif, M., E. Roeckner, U. Mikolajewicz, and R. Voss (2000), Tropical Stabilization of the
359 Thermohaline Circulation in a Greenhouse Warming Simulation, *Journal of Climate*,
360 *13*(11), 1809–1813, doi:10.1175/1520-0442(2000)0131809:L2.0.CO;2.
361 Levermann, A., P. U. Clark, B. Marzeion, G. A. Milne, D. Pollard, V. Radic, and
362 A. Robinson (2013), The multimillennial sea-level commitment of global warm-
363 ing, *Proceedings of the National Academy of Sciences*, *110*(34), 13,745–13,750, doi:

10.1073/pnas.1219414110.

Li, C., J.-S. Storch, and J. Marotzke (2013), Deep-ocean heat uptake and equilibrium climate response, *Climate Dynamics*, *40*(5-6), 1071–1086, doi:10.1007/s00382-012-1350-z.

Liang, X., C. Wunsch, P. Heimbach, and G. Forget (2015), Vertical Redistribution of Oceanic Heat Content, *Journal of Climate*, *28*(9), 3821–3833, doi:10.1175/JCLI-D-14-00550.1.

Llovel, W., J.K. Willis, F.W. Landerer, and I. Fukumori (2014), Deep-ocean contribution to sea level and energy budget not detectable over the past decade, *Nature Clim. Change*, doi:10.1038/nclimate2387.

Lowe, J. A., and J. M. Gregory (2006), Understanding projections of sea level rise in a Hadley Centre coupled climate model, *Journal of Geophysical Research: Oceans*, *111*(C11), doi:10.1029/2005JC003421.

Manabe, S., and K. Bryan (1985), CO_2-induced change in a coupled ocean-atmosphere model and its paleoclimatic implications, *Journal of Geophysical Research: Oceans*, *90*(C6), 11,689–11,707, doi:10.1029/JC090iC06p11689.

Manabe, S., and R. J. Stouffer (1994), Multiple-Century Response of a Coupled Ocean-Atmosphere Model to an Increase of Atmospheric Carbon Dioxide, *Journal of Climate*, *7*(1), 5–23, doi:10.1175/1520-0442(1994)0070005:MCROAC2.0.CO;2.

Marshall, J., J. R. Scott, K. C. Armour, J.-M. Campin, M. Kelley, and A. Romanou (2014), The ocean's role in the transient response of climate to abrupt greenhouse gas forcing, *Climate Dynamics*, *44*(7), 2287–2299, doi:10.1007/s00382-014-2308-0.

McDougall, T. J., D. R. Jackett, D. G. Wright, and R. Feistel (2003), Accurate and Computationally Efficient Algorithms for Potential Temperature and Density of Seawater, *Journal of Atmospheric and Oceanic Technology*, *20*(5), 730–741, doi:10.1175/1520-0426(2003)20730:AACEAF2.0.CO;2.

Meehl, G. A., T. Stocker, W. Collins, P. Friedlingstein, A. Gaye, J. Gregory, A. Kitoh, R. Knutti, J. Murphy, A. Noda, S. Raper, I. Watterson, A. Weaver, and Z.-C. Zhao (2007), Global climate projections, in *In: Climate Change 2007: The Physical Science Basis. Contribution of Working Group I to the Fourth Assessment Report of the Intergovernmental Panel on Climate Change*, edited by S. Solomon, D. Qin, M. Manning, Z. Chen, M. Marquis, K. Averyt, M. Tignor, and H. Miller, Cambridge University Press, Cambridge, United Kingdom and New York, NY, USA.

Melet, A., and B. Meyssignac (2015), Explaining the spread in global mean thermosteric sea level rise in CMIP5 climate models, *Journal of Climate*, doi:10.1175/JCLI-D-15-0200.1.

Opsteegh, J., R. Haarsma, F. Selten, and A. Kattenberg (2011), ECBILT: a dynamic alternative to mixed boundary conditions in ocean models, *Tellus A*, *50*(3).

Palter, J. B., S.M. Griffies, B.L. Samuels, E.D. Galbraith, A. Gnanadesikan, and A. Klocker (2014), The Deep Ocean Buoyancy Budget and Its Temporal Variability, *Journal of Climate*, *27*(2), doi:10.1175/JCLI-D-13-00016.1.

Pardaens, A. K., J. A. Lowe, S. Brown, R. J. Nicholls, and D. de Gusmão (2011), Sea-level rise and impacts projections under a future scenario with large greenhouse gas emission reductions, *Geophysical Research Letters*, *38*(12), doi:10.1029/2011GL047678.

Randerson, J. T., K. Lindsay, E. Munoz, W. Fu, J. K. Moore, F. M. Hoffman, N. M. Mahowald, and S. C. Doney (2015), Multicentury changes in ocean and land contributions to the climate-carbon feedback, *Global Biogeochemical Cycles*, *29*(6), 744–759, doi:10.1002/2014GB005079.

Rugenstein, M. A. A., M. Winton, R. J. Stouffer, S. M. Griffies, and R. Hallberg (2013), Northern high-latitude heat budget decomposition and transient warming, *Journal of Climate*, *26*(2), 609–621, doi:10.1175/JCLI-D-11-00695.1.

Sallée, J. B., E. Shuckburgh, N. Bruneau, A. J. S. Meijers, T. J. Bracegirdle, Z. Wang, and T. Roy (2013), Assessment of Southern Ocean water mass circulation and characteristics in CMIP5 models: Historical bias and forcing response, *Journal of Geophysical Research: Oceans*, *118*(4), 1830–1844, doi:10.1002/jgrc.20135.

Savin, S. M. (1977), The History of the Earth's Surface Temperature During the Past 100 Million Years, *Annual Review of Earth and Planetary Sciences*, *5*(1), 319–355, doi:10.1146/annurev.ea.05.050177.001535.

Schneider, S. H., and S. L. Thompson (1981), Atmospheric CO_2 and climate: Importance of the transient response, *Journal of Geophysical Research: Oceans*, *86*(C4), 3135–3147, doi:10.1029/JC086iC04p03135.

Stouffer, R., and S. Manabe (2003), Equilibrium response of thermohaline circulation to large changes in atmospheric CO_2 concentration, *Climate Dynamics*, *20*(7-8), 759–773, doi:10.1007/s00382-002-0302-4.

Voigt, S., A. S. Gale, and S. Flögel (2004), Midlatitude shelf seas in the Cenomanian-Turonian greenhouse world: Temperature evolution and North Atlantic circulation,

Paleoceanography, *19*(4), doi:10.1029/2004PA001015, pA4020.

Wunsch, C., and P. Heimbach (2014), Bidecadal Thermal Changes in the Abyssal Ocean, *Journal of Physical Oceanography*, *44*(8), 2013–2030, doi:10.1175/JPO-D-13-096.1.

Yamamoto, A., A. Abe-Ouchi, M. Shigemitsu, A. Oka, K. Takahashi, R. Ohgaito, and Y. Yamanaka (2015), Global deep ocean oxygenation by enhanced ventilation in the Southern Ocean under long-term global warming, *Global Biogeochemical Cycles*, *29*(10), 1801–1815, doi:10.1002/2015GB005181.

Yin, J. (2012), Century to multi-century sea level rise projections from CMIP5 models, *Geophysical Research Letters*, *39*(17), doi:10.1029/2012GL052947.

Yin, J., J. T. Overpeck, S. M. Griffies, A. Hu, J. L. Russell, and R. J. Stouffer (2011), Different magnitudes of projected subsurface ocean warming around Greenland and Antarctica, *Nature Geosci*, *4*(8), 524–528.

Zachos, J. C., M. Pagani, L. C. Sloan, E. Thomas, and K. Billups (2001), Trends, Rhythms, and Aberrations in Global Climate 65 Ma to Present, *Science*, *292*(5517), 686–693, doi:10.1126/science.1059412.

Zhu, J., Z. Liu, J. Zhang, and W. Liu (2014), AMOC response to global warming: dependence on the background climate and response timescale, *Climate Dynamics*, pp. 1–20, doi:10.1007/s00382-014-2165-x.

Zickfeld, K., M. Eby, A. J. Weaver, K. Alexander, E. Crespin, N. R. Edwards, A. V. Eliseev, G. Feulner, T. Fichefet, C. E. Forest, P. Friedlingstein, H. Goosse, P. B. Holden, F. Joos, M. Kawamiya, D. Kicklighter, H. Kienert, K. Matsumoto, I. I. Mokhov, E. Monier, S. M. Olsen, J. O. P. Pedersen, M. Perrette, G. Philippon-Berthier, A. Ridg-

well, A. Schlosser, T. Schneider Von Deimling, G. Shaffer, A. Sokolov, R. Spahni, M. Steinacher, K. Tachiiri, K. S. Tokos, M. Yoshimori, N. Zeng, and F. Zhao (2013), Long-Term Climate Change Commitment and Reversibility: An EMIC Intercomparison, *Journal of Climate*, *26*(16), 5782–5809, doi:10.1175/JCLI-D-12-00584.1.

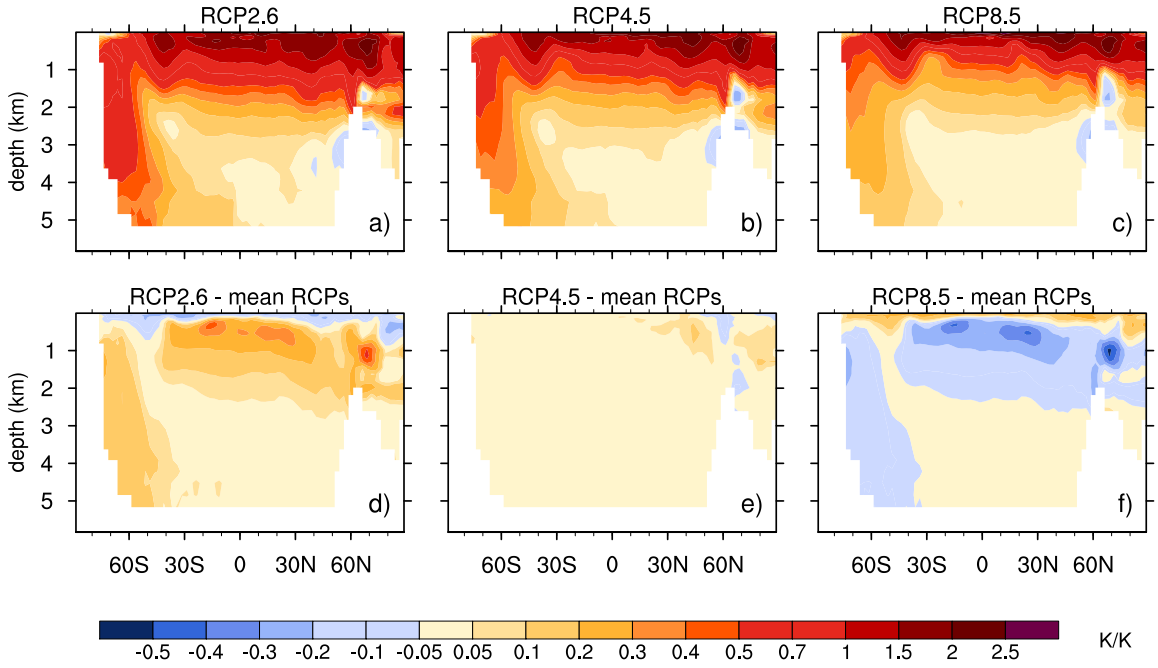

Figure 1. Zonal mean ocean temperature anomaly averaged over year 2081 to 2100 and normalized with the average ocean temperature of Representative Concentration Pathways (RCP) 2.6 (a), RCP4.5 (b), and RCP8.5 (c) of 14 CMIP5 Models, described in *Collins et al.* [2013], Figure 12.12. Differences between RCP2.6 (d), RCP4.5 (e), RCP8.5 (f) and the mean of the three RCPs. The color scale is not linear (around 0 and above .5). See SI Fig.1-3 for more details on each model.

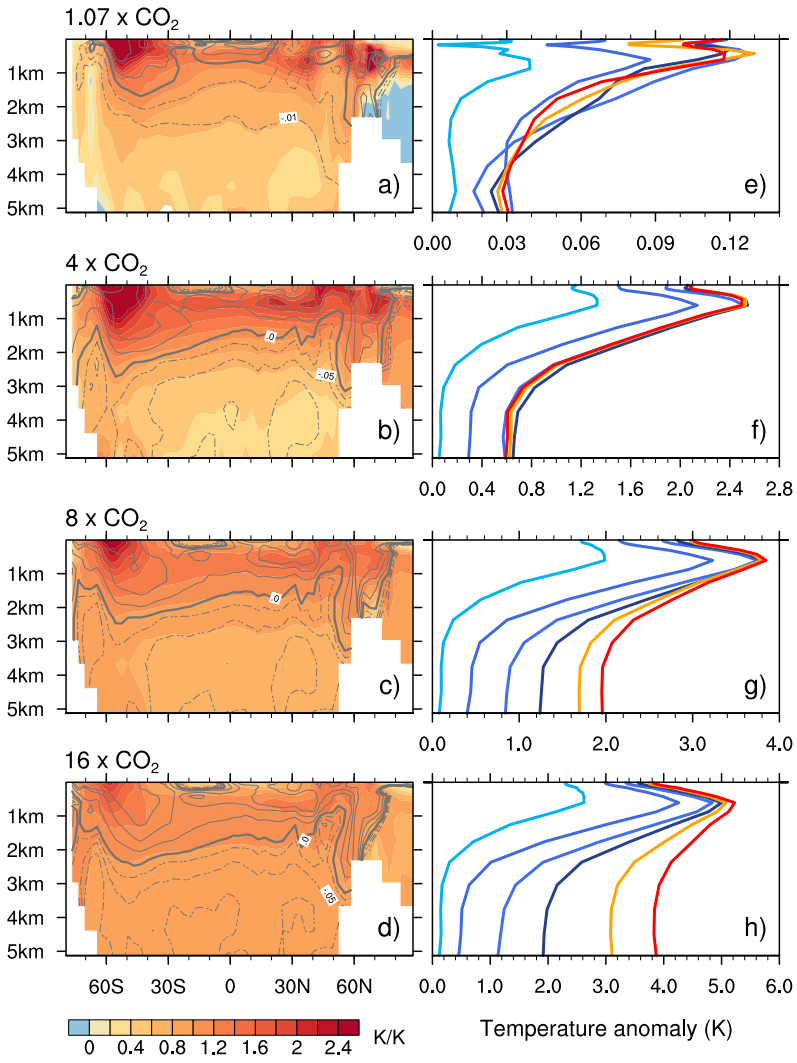

Figure 2. (a-d) Zonal average equilibrium (year 9000-10 000) ocean warming pattern for four forcing scenarios, normalized with the average ocean temperature of that time frame. Gray lines show salinity anomalies contours of -.075, -.05, -.025 (dashed) 0 (thick) and .05, .1, .15 psu unscaled. (e-h) Time evolution of global average warming at all depth for the same scenarios. Lines from light blue to dark blue to red indicate 100-year averages around year 100, 300, 600, 1000, 2000, and 9900 after the perturbation. Only the single long simulations are used for this figure. Scale for panel e-h changes.

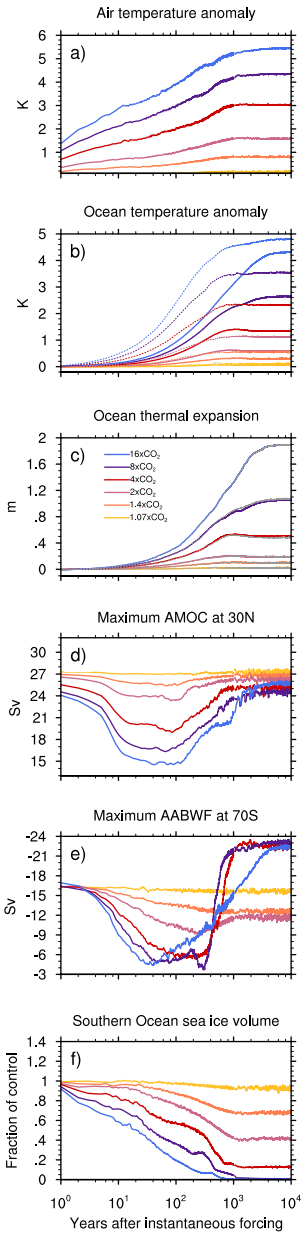

Figure 3. Time evolution of (a) global average surface air temperature anomaly, (b) global average ocean temperature anomaly for the whole (solid) and upper-most kilometer ocean (dashed), (c) global average ocean thermal expansion, (d) maximum Atlantic Meridional Overturning Circulation at 30° N, (e) Antarctic Bottom Water Formation, as maximum of overturning at 70° S, and (f) the sea ice volume, expressed as fraction of the control simulation value. In all panels, year 1-1000 is the annual and ensemble average; year 1000 – 10 000 is a 100 year running mean of one simulation for each forcing level.

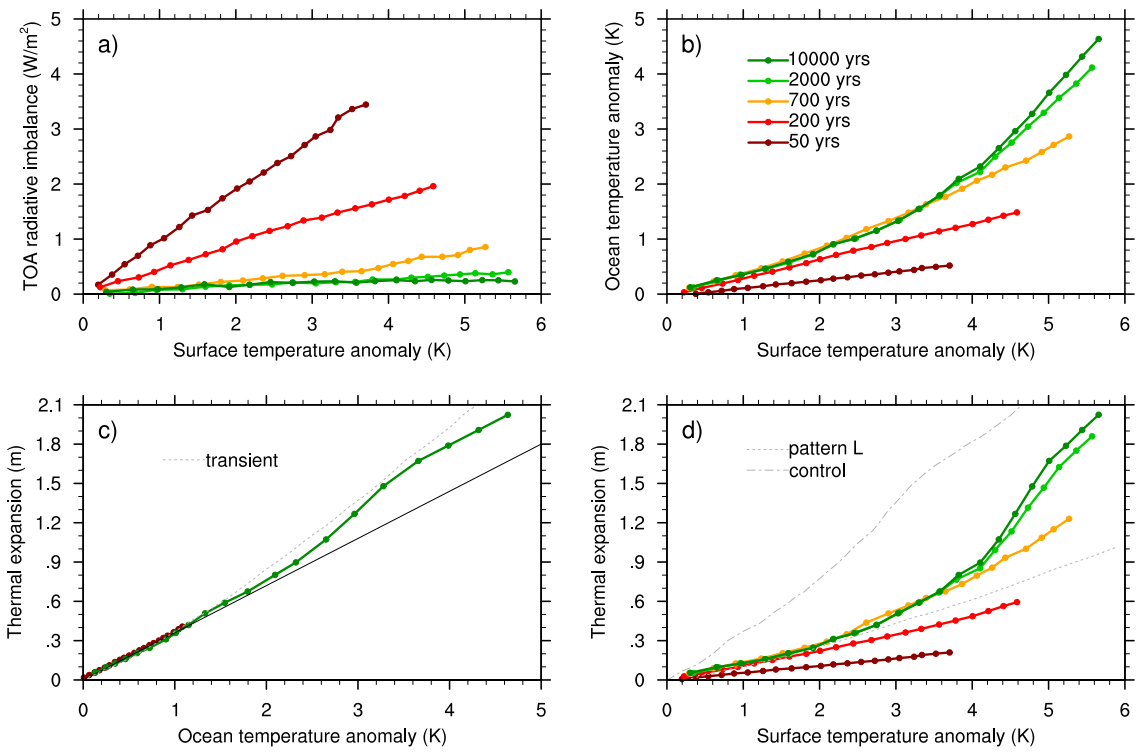

Figure 4. (a) Top of the Atmosphere (TOA) radiative imbalance versus global surface temperature anomalies averages around year 50, 200, 700, 2000, and 10 000. (b) Global ocean temperatures versus global surface temperature anomalies, (c) Global sea level rise due to thermal expansion versus global ocean temperature anomaly. Constructed thermal expansion without circulation change and a linear (black) or non-linear equation of state (gray). (d) Thermal expansion versus global surface temperature anomaly and constructed thermal expansion based on a pattern of equilibrated warming at 1.07xCO_2 (pattern L) and a uniform anomaly added to the control simulation pattern (control, both dashed gray).